Review of Scientific Instruments

PC software-based portable cyclic voltammetry system with PB-MCNT-GNPs-modified electrodes for *E. coli* detection

Cite as: Rev. Sci. Instrum. **91**, 014103 (2020); https://doi.org/10.1063/1.5113655
Submitted: 06 June 2019 . Accepted: 19 December 2019 . Published Online: 08 January 2020

Ying Xu, Yan Dai, Chao Li, Haijing Zhang, Miao Guo, and Yong Yang

Review of Scientific Instruments ARTICLE scitation.org/journal/rsi

PC software-based portable cyclic voltammetry system with PB-MCNT-GNPs-modified electrodes for *E. coli* detection

Cite as: Rev. Sci. Instrum. 91, 014103 (2020); doi: 10.1063/1.5113655
Submitted: 6 June 2019 • Accepted: 19 December 2019 •
Published Online: 8 January 2020

Ying Xu,[a] Yan Dai, Chao Li, Haijing Zhang, Miao Guo, and Yong Yang

AFFILIATIONS

College of Automation, Hangzhou Dianzi University, Xiasha Higher Education Zone, Hangzhou 310018, Zhejiang Province, China

[a]Author to whom correspondence should be addressed: 635419441@qq.com and xuyingxy@hdu.edu.cn

ABSTRACT

PC software-based portable cyclic voltammetry (PCV) systems have the advantages of portability, high performance, and real-time detection. In this paper, the PCV system used cyclic voltammetry (CV) as the main detection and analysis method and contained the following components: a three-electrode unit, a portable potentiostat, and PC software. The PC software was used as the system control and display, and a dynamic peak position adjustment (DPPA) algorithm for *E. coli* measurements based on thick biofilm modification on electrodes was designed especially for this system to realize the real-time correspondence between the measured results and the modified electrodes. The performance test results obtained by setting different detection parameters in the PCV system were compared with those of commercial electrochemical workstations. The difference was less than 4.99%, with a relative standard deviation less than 0.20%. An electrochemical biosensor based on a Prussian blue-multiwalled carbon nanotube-gold nanoparticle composite was developed for *E. coli* detection. After constructing an antibody-BSA-*E. coli* electrode modification on the sensor, experimental data processed by the DPPA algorithm showed that the logarithm ($\lg Df_{E.coli}$) of the *E. coli* dilution factor and the peak current response had a linear relationship. The PCV system could quickly and accurately detect *E. coli* concentrations with dynamic adjustment algorithms for biofilm-modified electrodes. Furthermore, the system could detect the electrochemical activities of various high-sensitivity biomolecules, showing great detection potential for on-site monitoring and meeting the requirements of real-time and portable detection in various food safety fields.

I. INTRODUCTION

Electrochemical detection is widely used in various analyses and detection fields for environmental monitoring, medical health diagnosis, and food safety monitoring and has the advantages of low measurement limits, good repeatability, and direct feedback of electrical signals.[1–3] The potentiostat is indispensable in electrochemical analysis and an important interface of electrochemical detection device for various three-electrode units.[4] Potentiostat research is still in the preliminary development and application stage, and large and complicated electrochemical workstations are still required for related experiments.[5] With the continuous development of detection technology and the maturity of integrated electronic technology, some progress has been made in the development of portable potentiostats. Huang *et al.* reported an integrated potentiostat with a 10-ms sampling interval.[6] Nevertheless, measurements with sampling intervals of less than 1 ms are often suggested,[7] and a real-time potentiostat with 4 channels to amplify the current response was reported by Zhang *et al.*[8] However, inadequate amplification accuracy may result in measurement inaccuracy. Therefore, to ensure accuracy and stability, a potentiostat developed with intelligence and portability is required.

Common electrochemical detection methods include chronoamperometry (CA),[9] square wave voltammetry (SWV),[10] differential pulse voltammetry (DPV),[11] and electrochemical impedance spectroscopy (EIS).[12] Among many electrochemical detection methods, cyclic voltammetry (CV) under linear voltage scanning excitation has been widely used in chemical and biological fields.[13] Data acquisition and processing systems have long been generally designed based on the system architecture of PCs and microcontroller units (MCUs).[14] The intelligence, efficiency, and strong compatibility of PC software render it advantageous

for collecting, online processing, and calculating large and complex electrochemical detection data.[15]

One of the main applications of potentiostat detection systems is the rapid, effective, and accurate measurement of a variety of microorganisms, including bacteria testing in food safety monitoring of common bacteria such as *Escherichia*, *Staphylococcus aureus*, and *Salmonella*.[16–19] *E. coli* is a food-borne bacterium that is abundantly present in the intestines and feces of warm-blooded animals.[20] Common *E. coli* detection methods include plate counting,[21,22] enzyme-linked immunosorbent assay (ELISA),[22] and chemiluminescence (CL).[23] The research on highly portable, low-power, and low-cost electrochemical detection methods for biological cell detection technology is nearly half a century old, beginning with the generation of the first glucose oxidase electrochemical electrode.[24] Currently, the combination of electrochemical detection technology and biological components is attempted. In particular, a method of electrochemical detection for *E. coli* based on nanomaterial has attracted extensive attention.[25] However, due to the instability of electrode modifications based on nanomaterials, both electrode modification methods and measuring instruments with appropriate algorithms are essential.

At present, there are many instruments based on smartphones for electrochemical measurements. Dou *et al.* reported a biosensing system for the detection of clenbuterol (CLB) using a homemade mobile electrochemical device with an electric field-driven acceleration strategy,[26] and Sun *et al.* reported a low-power potentiostat that harvested power from a smartphone and conducted cyclic voltammetry experiments with potassium ferro-/ferricyanide solution.[27] However, for complex thick biofilm-modified electrodes and the corresponding application measurements (e.g., *E. coli*, protein, etc.), when the biofilm on electrodes is thicker and the charge transfer process is more complex, it is necessary to adopt dynamic filtering and calibration algorithms based on PC tablets and to extract and process signals according to the system measurements, also including online algorithms of removing gross errors and calibrating baselines. Therefore, compared with an application based on a smartphone, the PC software based on a PC terminal can realize online data processing that is compatible with various formats of detection data, higher stability, and real-time data transmission capability.

In this paper, a PC software-based portable cyclic voltammetry (PCV) system was designed, and a modification method for the electrode based on the system was used for the portable detection of electroactive biomolecules. The system was composed of a three-electrode unit, a portable potentiostat, and PC software. The PC software was used as the system control and display by setting the communication and detection parameters, realizing online data processing, displaying CV curves and linear standard curves in real time, and calculating peak information. In addition, a dynamic peak position adjustment (DPPA) algorithm suitable for *E. coli* measurements based on thick biofilm was designed specifically. As a verification, a Prussian blue-multiwalled carbon nanotube-gold nanoparticle (PB-MCNT-GNPs) composite was modified on a bare gold electrode and employed as a sensor to detect *E. coli* by depositing an antibody-BSA-*E. coli* electrode-modified layer. Therefore, the PC software-based PCV system could perform varied online calibrations and carry out the fast and accurate detection of biomolecules with PB-MCNT-GNPs-modified electrodes for on-site monitoring.

II. MATERIALS AND METHODS

A. The design of the portable potentiostat

A portable potentiostat was used to detect and transmit electronic information to the PC software. The potentiostat was composed of the following four modules: a signal conversion module, control module (STM32F103C8T6), Bluetooth module (HC-06), and power unit. The signal conversion module consisted of a DAC submodule (16 bits DAC, AD5760, ADI), AFE submodule (sensor analog front-end, ADA4350, ADI), and ADC submodule (24 bits ADC, AD7172-2, ADI). STM32F103C8T6 was used as the MCU of the portable potentiostat to control the DAC to output the triangular wave linear voltage excitation signals to the biosensor, the ADC was used to collect the response current signal from the biosensor, and the HC-06 was to transmit voltage-current signals to the PC software. In the process of signal conversion, the AFE was used for automatic gain selection. The power unit provided voltages for each module of the portable potentiostat. The above four modules were placed into a 4.06 × 3.6 in. printed circuit board (PCB) for CV performance testing and *E. coli* detection application testing, and the PCB provided three wired interfaces (the three-electrode interface) and one wireless interface (Bluetooth communication).

B. The design of the PC software

The PC software was used as the control and display of the PCV system. It communicated with the portable potentiostat via Bluetooth to transmit data and commands to control CV measurements, process the real-time data, and plot the cyclic voltammograms and linear standard curves. The PC software was composed of the following four modules: a communication parameter setting module, detection parameter setting module, online data processing algorithm module, and real-time display module. During the online data processing, the DPPA algorithm was implemented specifically for *E. coli* measurement in the PCV system. By importing multiple CV curves under different electrode modifications and adjusting the horizontal peak position of the curves to a similar horizontal peak position as the reference curve, the measurement will be simple and effective. More details of the algorithm are introduced in Sec. III B [the PC software and DPPA algorithm flow chart is shown in Fig. S1(a) of the supplementary material]. The DPPA algorithm simplifies the comparison among the peak values of CV curves and the calculation of standard linearity under different electrode modification measurements, especially for *E. coli* measurement. Furthermore, the algorithm could realize the real-time correspondence between the measured results and the modified electrodes. Some other online calibrations in the online data processing algorithm module were designed to further optimize measurement results, such as denoising the coarse noise by the quantile method and curve fitting by the least square method. Compared with smartphone-based applications, PC-based detection software can record, import, and analyze more electrochemical data and realize online data processing due to its powerful computing accuracy and stability.

C. The design of the PC software-based PCV system

The PC software-based PCV system consisted of a three-electrode unit, a portable potentiostat, and PC software. The three-electrode unit was modified by biomacromolecules and specific sensitive substance. The electrochemical reactions on the electrodes were converted into analog electrical signals, which were amplified, collected, and converted into digital signals by the portable potentiostat. Finally, the signals were transmitted to the PC software by the portable potentiostat's Bluetooth module. After online data processing with the PC software, the calibrated CV curve and the linear standard curve could be displayed on the PC software interface.

D. Performance testing of the PC software-based PCV system

1. Baseline testing

Baseline drift is a common phenomenon in analytical chemistry and leads to specific difficulties in data processing, especially for quantitative analysis.[28] Basically, the electrochemical response signal of the three-electrode unit is caused by the change of the solution impedance (equivalent to the change of the ion concentration in the solution) between the electrodes. According to the equivalent model of the electrolytic cell circuit, the three-electrode circuit can be simplified to a pure resistance equivalent model when the electrolytic reaction is stable.[29,30] Therefore, the solution impedance between the three electrodes is simplified as the pure resistance. By changing the value of the solution resistance R_{FW} between the reference electrode (RE) and the working electrode (WE) to match 6 gains (1 k, 5 k, 10 k, 50 k, 100 k, and 1M) of the AFE, the portable potentiostat measured the baseline under these 6 gains. When every point of the baseline meets the following characteristic:

$$I_{out} = {}^{V_{in}}/_{R_{FW}}, \tag{1}$$

the baseline calibration was realized.

2. Accuracy and stability testing

The three-electrode unit and the redox couple solution at different concentrations under different scan rates were applied for the accuracy and stability performance tests with the PC software-based PCV system. Ag/AgCl electrodes, gold electrodes with a diameter of 1 mm, and platinum wire electrodes were used as the RE, WE, and counter electrode (CE), respectively. The PCV system was tested with 3 different scan rates (10 mV/s, 20 mV/s, and 50 mV/s), and the redox couple solution was measured at 5 different concentrations (5 mM, 10 mM, 20 mM, 50 mM, and 100 mM). Some parameters were fixed during measurement, such as the excitation voltage (V_{in}), the sample interval, and the number of measurements.

E. The method of electrode modification based on the PB-MCNT-GNPs composite

A biosensor based on the PB-MCNT-GNPs composite was constructed on the gold electrode. First, the carboxylated MCNT was dispersed into the $FeCl_3$ solution. Then, the potassium ferrocyanide (PB) solution was added to the solution dropwise during the stirring process. Stable PB-MCNT dispersions were prepared by a supersonic method. After centrifugation, the precipitates were dispersed into the chitosan aqueous solution to obtain amino groups on PB-MCNT. Then, after centrifugation, the excess chitosan was removed, the gold colloid was added, the solution was stirred, and the nanocomposites were obtained. The nanocomposites were dispersed in the deionized water to obtain the PB-MCNT-GNPs composite. Finally, the PB-MCNT-GNPs composite was deposited on the surface of the treated gold electrode and irradiated by an infrared lamp to dry the composite and construct the biosensor interface.[25,31]

F. The PC software-based PCV system for *E. coli* detection

After the biosensor electrode based on the PB-MCNT-GNPs composite was constructed, antibodies against *E. coli* (10 μl, 1 mg/ml) were added to the biosensor surface at the super-clean platform, dried for 1 h, immersed in BSA (10 μl, 0.1%), and then washed with PBS. Finally, electrodes were incubated in six different concentrations of *E. coli* solutions (0.1 ml, concentration was 1×10^9 cfu/ml, dilution factors were ×2, ×4, ×8, ×10, ×20, and ×40) for 1 h before *E. coli* measurement.[29] *E. coli* (DH5α) was obtained from the Life Science Institute of Zhejiang University (Hangzhou, China). *E. coli* antibody (anti-*E. coli* rabbit polyclonal antibody) was purchased from Sangon Biotech Co., Ltd. (Shanghai, China). The *E. coli* stain adopted in this paper was DH5α which is nonpathogenic and mainly used in gene cloning. It was used in the experiment to verify the feasibility of the PCV system. All chemical reagents used in this work were of analytical grade and were used as received. All aqueous solutions were prepared using ultrapure water (Aquelix 5, Merck Millipore, Massachusetts, USA).

The three-electrode unit, which was combined with *E. coli* on WE, was connected with the three wired interfaces of the portable potentiostat for electrochemical measurements. The detection parameters for each group of *E. coli* measurement, such as the excitation voltage range from −0.2 to 0.6 V, a scan rate of 50 mV/s, a sample interval of 0.001 V, and number of measurements (n = 10), were set by the PC software.

III. RESULTS AND DISCUSSION

A. The performance of the PC software-based PCV system

The whole system was composed of the following components: a three-electrode unit, portable potentiostat, and PC software [Fig. 1(a)]. The three-electrode unit was modified with the PB-MCNT-GNPs composite and sensitive sensing substance for the system to act as the biosensor for CV detection. As the core component of the system, the portable potentiostat circuit was designed with a small-scale PCB board and was used to detect and transmit electrochemical signal to the PC software.

When running a CV detecting program, the three-electrode unit, portable potentiostat, and PC software were connected as shown in Fig. 1(a). The PC software was used to set the communication and detection parameters, realize online data processing, display CV curves and linear standard curves in real time, and calculate peak information. As shown in Fig. 1(b), a Bluetooth connection button was used to connect the portable potentiostat via Bluetooth by selecting a communication port. Users can set the detection parameters (including the initial voltage, final voltage, scan rate, scan

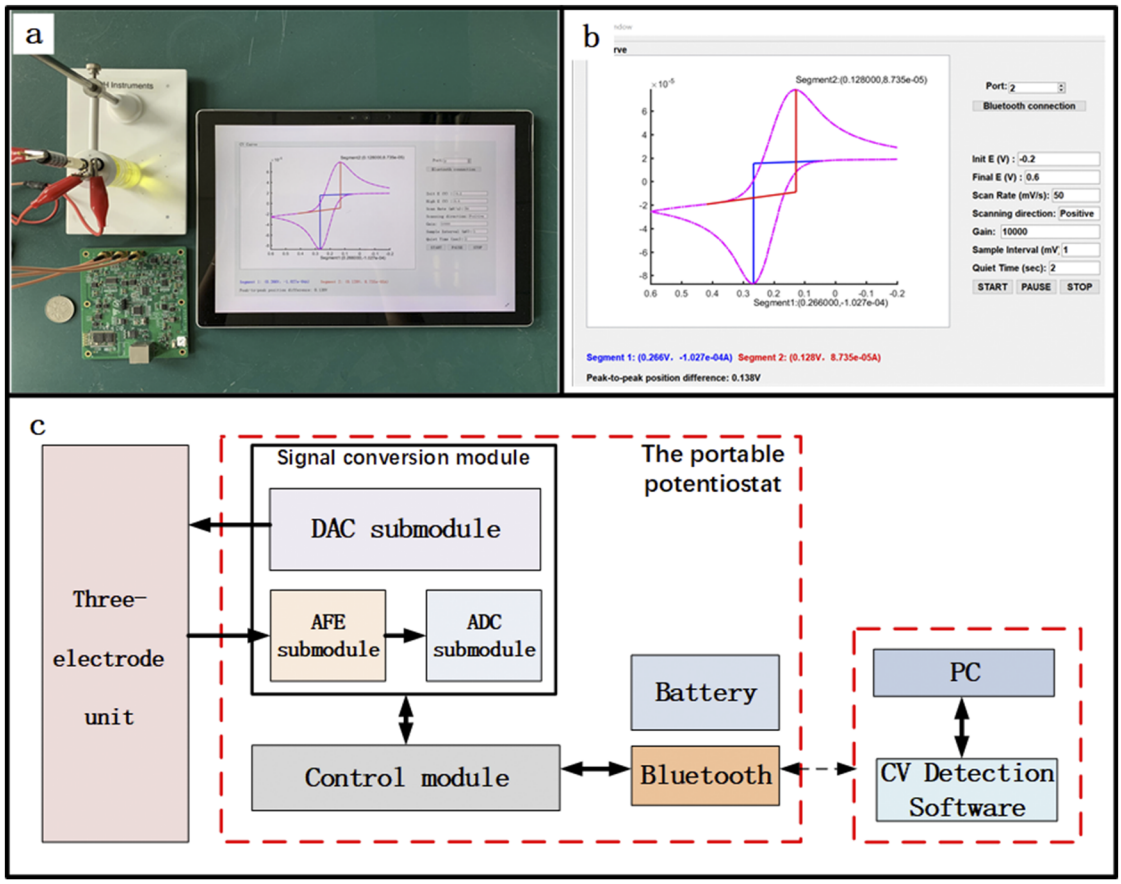

FIG. 1. Schematic diagram and design of the PC software-based PCV system. (a) Image of the portable potentiostat connected to the three-electrode unit and the PC software. (b) The detection interface of the PC software on a surface (Surface Pro 6, Microsoft). (c) A schematic diagram of the PC software-based PCV system.

direction, gain, sample interval, and quiet time) for CV measurements and click the START button to start sending commands to the portable potentiostat and receiving data to plot the CV curve in real time. At the same time, the scan rate is adjustable in the range from 10 to 100 mV/s, and the voltage range is adjustable from −1 to 1 V. The PAUSE and STOP buttons were used to suspend and end the CV measurements, respectively. The peak information of the CV curve was calculated and immediately displayed by the online data processing module and real-time display module of the PC software after the test finished. In addition, by loading multiple measurements and the DPPA algorithm, the PC software could adjust the peak position dynamically for thick biofilm modification measurements. By importing the test data from the commercial electrochemical workstation (CHI760E, CH Instruments, Inc., USA) under the same experimental conditions, the peak-seeking accuracy of the PC software was evaluated. The error of the peak position was 0.001 V, and the error of the peak value was 1.19 μA, which showed that the peak-seeking accuracy of the PC software was quite high.

The operational process of the PCV system is shown in detail in Fig. 1(c), and the working of each module was interrelated and coordinated. As shown in Fig. 1, the PCV system with its miniature, portable and low-cost hardware, and simple operating software solved the disadvantages of the commercial electrochemical workstations, which are heavy, expensive, and unsuitable for on-site detection.

1. Baseline test results

The three-electrode unit was used as the electrochemical sensor of the PCV system for electrochemical analysis and detection. As shown in Fig. 2(a), the unit included RE, CE, WE, and electrolyte solution, through which RE provided the reference potential, CE provided the current output, and WE worked as the measuring electrode. The electrolyte solution was stimulated by a voltage signal to produce a redox reaction and form a weak current. The current signal had a specific relationship with the concentration of the measured substance; thus, if a peak current could be measured, the concentration of the measured substance could be calculated. According to the circuit equivalence principle of the electrolytic cell, the three-electrode model in the electrolytic cell could be equivalent to that as Fig. 2(b) shows.

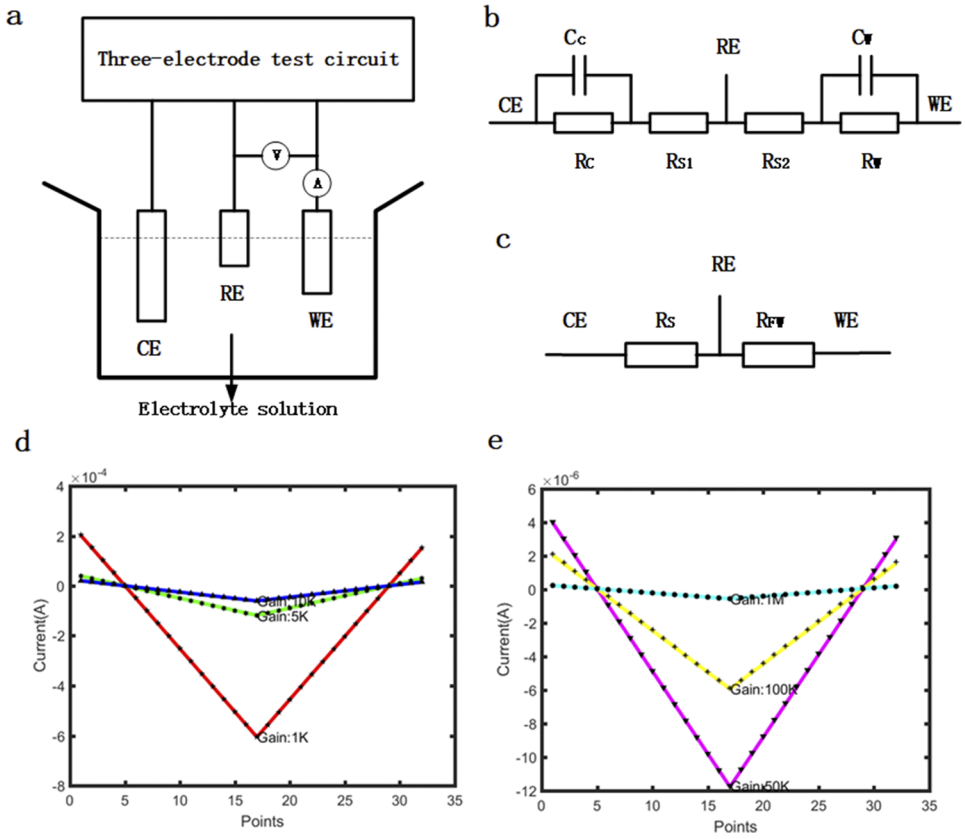

FIG. 2. Schematic diagram of the three-electrode unit and the three-electrode circuit equivalent model, and the results of the baseline tested by the CHI760E (solid line curves) and the PCV system (dotted line curves). (a) Schematic diagram of the three-electrode unit. (b) Three-electrode equivalent impedance model. (c) Pure resistance equivalent model. (d) Baseline test results with gains of 1 k, 5 k, and 10 k. (e) Baseline test results with gains of 50 k, 100 k, and 1M.

Figure 2(b) was further simplified to the pure resistance equivalent model in Fig. 2(c), which was used to carry out baseline tests. As shown in Fig. 2(c), R_S is equivalent to the resistance of the solution between WE and CE, and R_{FW} is the equivalent resistance on the contact surface between WE and the electrolyte. Six gains (1 k, 5 k, 10 k, 50 k, 100 kΩ, and 1M) generated by AFE of the portable potentiostat were matched with R_{FW} (1 kΩ, 5 kΩ, 10 kΩ, 50 kΩ, 100 kΩ, and 1 MΩ) in the pure resistance equivalent model. Six groups of measurements were performed by CHI760E and the PCV system. As shown in Figs. 2(d) and 2(e), the results of the PCV system coincided well with those of CHI760E. The relative deviation (RD) of the baseline test results was less than 0.98%, and the relative standard deviation (RSD) was less than 0.12%, indicating that the baseline of the PCV system under 6 gain conditions was effectively calibrated, and the lower measurement limit could reach the microampere level (10^{-6}).

2. Accuracy and stability testing

To test the performance of the PCV system, potassium ferricyanide/potassium ferrocyanide redox couples were selected to perform accuracy and stability testing. The performance test results were compared with those of CHI760E in different situations. As shown in Fig. 3(a), the CV test curves of the redox couples with different concentrations (5 mM, 10 mM, 20 mM, 50 mM, and 100 mM) were obtained with the PCV system and CHI760E at a constant scan speed of 50 mV/s. As shown in Fig. 3(b), the CV test curves of the 100 mM redox couple solution were obtained with the PCV system and CHI760E at different scan speeds (10 mV/s, 20 mV/s, and 50 mV/s). As a result, the CV curves obtained by the PCV system were very similar to those of CHI760E, especially the baseline and the peak positions, indicating that this portable wireless PCV system could accurately measure CV currents and potentials in different situations.

Figure 3(c) shows three CV curves obtained under 5 mM, 10 mM, and 20 mM redox couple solutions at 10 measurements on one electrode to measure the stability of the PCV system. The 10 CV curves of the same concentration almost coincided, and the results of the PC software-based PCV system were very stable. To further illustrate the stability of the PCV system, the mean and SD of the peak values of the measurement results in Fig. 3(c) were calculated, and the mean ± SD statistical chart is shown in Fig. 3(d). As illustrated in Fig. 3(d), the mean ± SD values of the 5 mM solution measured by the PCV system and CHI760E were $5.11 \times 10^{-6} \pm 1.06 \times 10^{-8}$ A and $5.05 \times 10^{-6} \pm 1.26 \times 10^{-8}$ A, respectively. The mean ± SD values of the 10 mM solution measured by the PCV system and CHI760E were $8.64 \times 10^{-6} \pm 1.72 \times 10^{-7}$ A and $8.35 \times 10^{-6} \pm 1.29 \times 10^{-7}$ A, respectively. The mean ± SD values of the 20 mM solution in the PCV system and CHI760E were $2.005 \times 10^{-5} \pm 2.56 \times 10^{-8}$ A and $1.966 \times 10^{-5} \pm 2.27 \times 10^{-8}$ A, respectively. The peak current of the PC software-based PCV system matched well with that of the CHI760E system, and the SD level was similar to that of the commercial platform. In addition, the

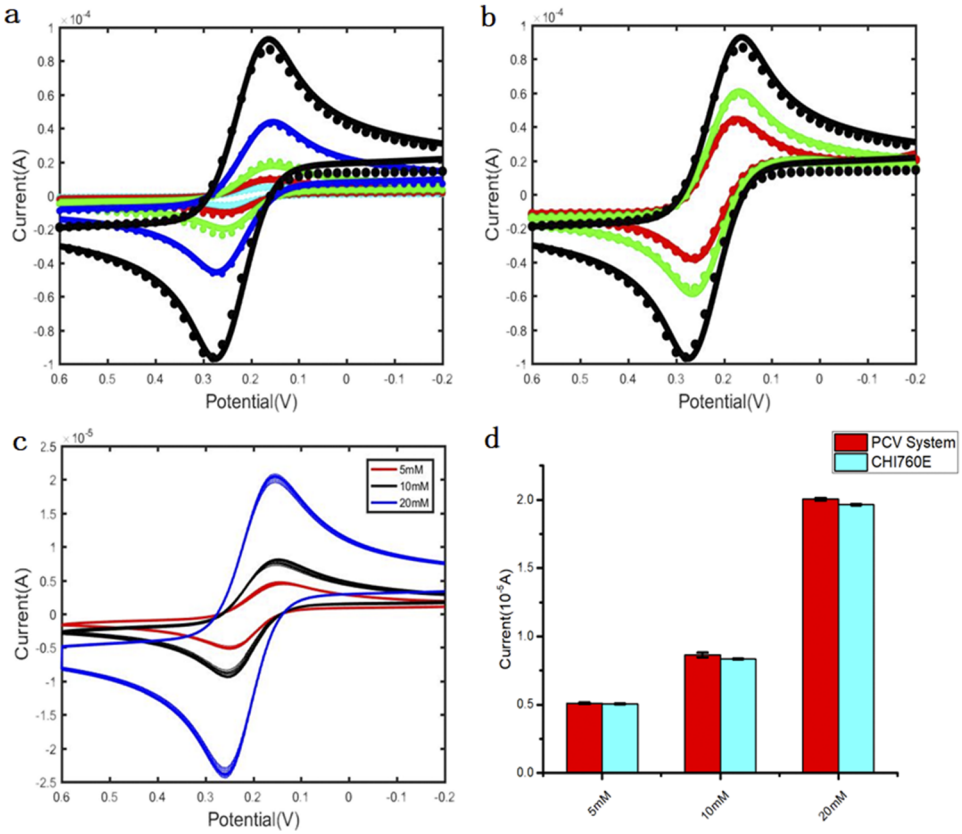

FIG. 3. Accuracy and stability CV test results of the CHI760E (solid line curves) and PCV systems (dotted line curves). (a) CV curves of redox couples at different concentrations (black: 100 mM, blue: 50 mM, green: 20 mM, red: 10 mM, and cyan: 5 mM) with a scan rate of 50 mV/s. (b) CV curves of the 100 mM redox couple solution at different scan rates (black: 50 mV/s, green: 20 mV/s, and red: 10 mV/s). (c) Stability of CV curves under 5 mM, 10 mM, and 20 mM redox couple solutions at a scan rate of 50 mV/s (10 measurements on one electrode, n = 10). (d) Statistics chart (mean ± SD) of the peak currents under different concentrations of the redox couple solutions by the PCV system and CHI760E.

mean values (n = 10) of the measuring results by the PCV system at three concentrations were linearly fitted with the results of CHI760E, and the regression equation, correlation coefficient R, and P values were calculated. The fitting results showed that the correlation coefficients R between the measurement results of the PCV system and CHI760E at three concentrations were greater than 0.998, and all the P values were less than 0.001 with the significance at 0.01 level. The specific comparison results indicated that the measuring result of the PCV system in solutions of potassium ferricyanide/potassium ferrocyanide redox couples under different concentrations has a fine linear relationship with that of CHI760E.

The accuracy and stability test results are detailed in numerical form in Table I. At the scan rate of 10 mV/s, the difference was 4.99%, which was the largest among all scan rates. In the different concentration tests, the difference between CHI760E and the PCV system was quite small—less than 3.77%. In summary, according to the data in the table, the accuracy and stability of the PCV system were ideal. Compared with CHI760E, the difference of the PCV system was less than 4.99%, and the RSD was less than 0.20%, which showed that the performance of the PCV system was comparable to that of commercial electrochemical platforms, and the system had great detection potential because of its low cost, portability, and high

TABLE I. Accuracy and stability tests for the PC software-based PCV system at different scan rates with different concentrations of redox couples.

		Scan rate (mV/s)			Concentration of the redox couple (mM)					
Peak current		10	20	50	5	10	10 (3σ)	20	50	100
CHI760E	Current value (μA)	54.54	71.96	104.81	5.05	8.35	8.35	19.66	47.69	104.81
PCV system	Mean value (μA)	51.82	69.25	103.62	5.11	8.64	8.48	20.05	45.89	103.62
	Difference (%)	4.99	3.77	1.14	1.18	3.47	1.56	1.98	3.77	1.14
	SD (10^{-8})	9.01	7.69	6.37	1.06	17.15	1.52	2.56	2.43	6.37
	RSD (%)	0.17	0.11	0.06	0.2	1.98	0.18	0.13	0.05	0.06

performance. Compared with smartphone-based CV detectors, the system could not only realize online data processing but also normalize prediction and comparison of measurements with different electrode modifications. Compared with other PC software-based CV detectors, the PCV system could perform sensitive, accurate, and steady CV detection and offered a more effective and convenient measurement method for *E. coli* measurement based on thick biofilm modification (detail in Sec. III B). With these advantages, the PCV system met the current market requirements for on-site electrochemical detection and also contributed to the development of other biomacromolecule measurements based on thick biofilm modification.

B. The modification and characterization of the three-electrode unit

Figure 4(a) shows the electrode modification process on the three-electrode unit. First, the PB-MCNT-GNPs composite was dropped onto the bare gold electrode and used for fabrication of the PB-MCNT-GNPs modified electrode in the PC software-based PCV system. The PB-MCNT-GNPs composite could enhance the electron transfer efficiency and electrode stability. Then, the PB-MCNT-GNPs-modified electrode was further sequentially deposited with antibodies and the BSA layer. Finally, *E. coli* solutions with different concentrations were added to perform CV tests. Figure 4(b)

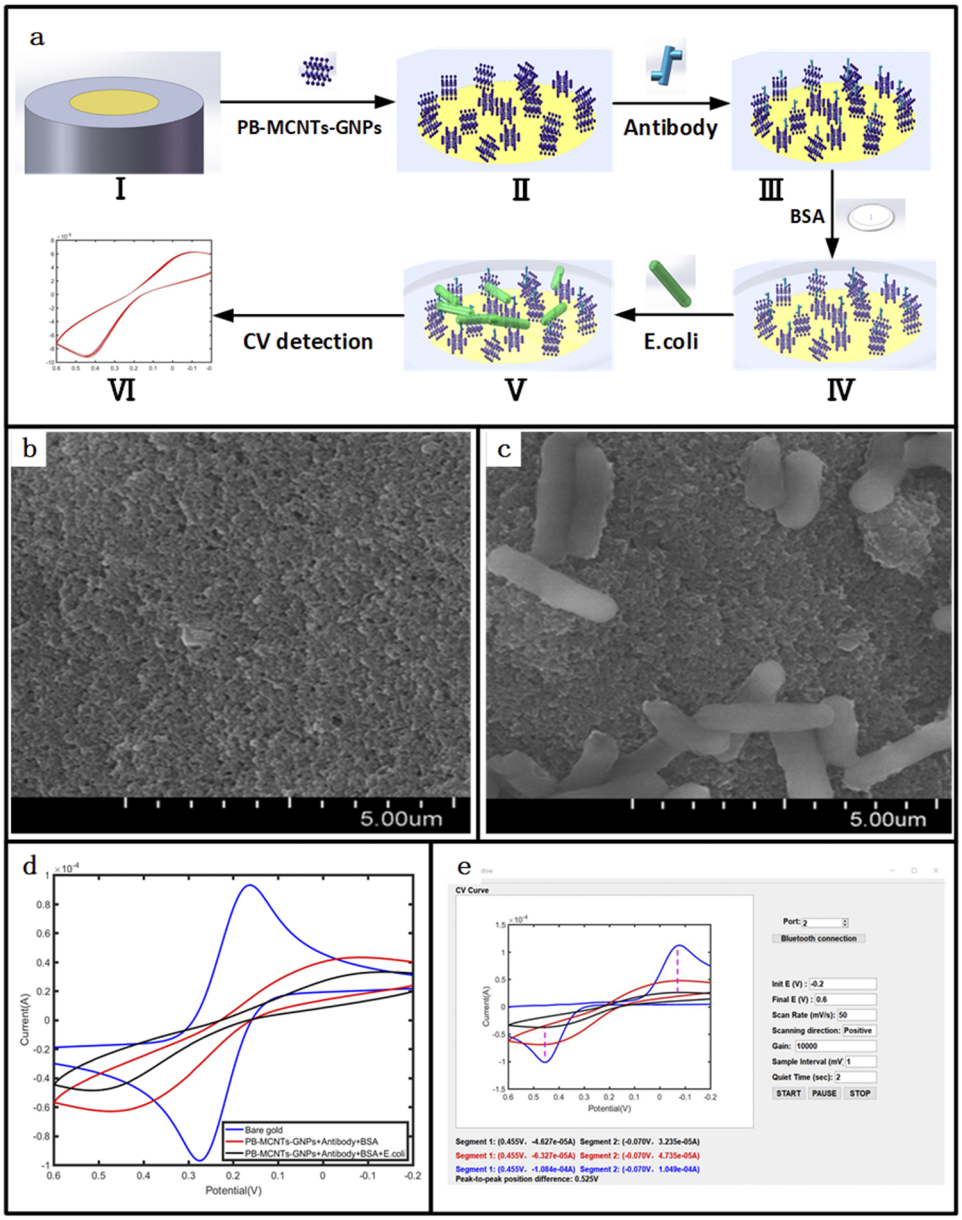

FIG. 4. The modification and characterization of the three-electrode unit. (a) The process of electrode modification. (b) SEM image of the modified layer without *E. coli*. (c) SEM image of the modified layer with *E. coli*. (d) The characterization of modified electrodes. (e) CV curves processed by the DPPA algorithm in the PC software.

is shown as a comparison to Fig. 4(c). Figure 4(b) shows the SEM image of the modified biosensor surface without *E. coli*. The surface of the modified electrode was roughly distributed in a uniform manner. Figure 4(c) shows the SEM image of the modified biosensor surface with *E. coli*. It was clear that *E. coli* was specifically and successfully attached on the modified biosensor surface.

The process of electrode modifications was characterized by CV curves, which were measured by the PCV system and are shown in Fig. 4(d). Figure 4(d) shows that the peak value of the CV curve (blue curve) of the bare gold electrode was the highest since there were no biological molecules or other layers hindering the electrochemical reaction. The peak value of the CV curve (red curve) with BSA and antibody deposited on the sensor surface decreased significantly because although PB-MCNT-GNPs promoted electron transport, BSA served as a blocking buffer that not only protected the antibodies but also blocked gold nanoparticle sites from binding to other material. The peak value of the CV curve (black curve) caused by PB-MCNT-GNPs + antibody + BSA + *E. coli* electrode modification was smaller than that of the red curve, which was due to further impediment of electron transfer by biomacromolecule substances. In addition, Fig. 4(d) shows that the peak positions of the three CV curves were not aligned. This change is because the thicker biofilm resulted in slower electric charge transfer at the sensor interface. This phenomenon showed that the modification of the biomacromolecule material on the electrode would lead to a decrease in the electron transfer rate and that the peak value of the CV curve was the key parameter for calculating the concentration of *E. coli*. The peaks of the three CV curves under different electrode modifications were adjusted to similar positions by the DPPA algorithm (Fig. S1). The main modules can be divided into the following steps: First, the peak positions of all of the curves were calculated, and the measurement result of the slowest transmission rate caused by the thickest modification layer was chosen as the reference curve. Second, the fitting equations of the remaining curves were obtained by genetic algorithm fitting. To optimize the fitting waveform, we chose 10% as the empirical value. When the baseline slopes of other curves exceeded that value, the shapes of the curves would be optimized according to the fitting equation and baseline slope until they converged to the threshold. Then, we kept the peak value of each curve unchanged and moved the voltage peak position of each fitting curve to the reference curve. Finally, the curves were interpolated, and the redundant points were deleted within the voltage range. Figure 4(e) shows that the relative peak value of the curves after DPPA was more obvious and analyzable, which was more conducive to the preliminary rapid prediction of the experimental results for the different surface-modified electrodes.

C. *E. coli* detection using the PC software-based PCV system

As shown in Fig. 5(a), the CV detection curves of *E. coli* solutions with different dilution factors [×2 (cyan), ×4 (black), ×8 (green), ×10 (red), ×20 (blue), and ×40 (magenta)] were measured and plotted in their entirety. In Fig. 5(a), the larger the dilution factor, the larger the absolute value of the peak current response (PCR). This is because a larger dilution factor results in a smaller amount of *E. coli* on the surface of the electrode, which agreed with the relationship between the thick biofilm and the electric charge transfer mentioned above. Furthermore, although PB-MCNT-GNPs promoted electron transport compared with bare electrode, *E. coli* antibodies were effectively bound by the PB-MCNT-GNPs composite modified on the electrode surface, which increased the attached amount of *E. coli*, thereby decreasing the current response. The repeatability and stability of *E. coli* CV measurements based on thick biofilm sensors under the same experimental conditions were ideal (10 measurements on each electrode, n = 10).

The electrochemical responses of the sensor in *E. coli* solutions with different concentrations were determined by the PCV system, and the standard equation for the relationship between the *E. coli* concentration and the PCR of the oxidation peaks was calculated. As shown in Fig. 5(b), the horizontal coordinate was the logarithmic value (lg2, lg4, lg8, lg10, lg20, and lg40) of the *E. coli* dilution factor, and the longitudinal coordinate was the mean value of the corresponding PCR. At the same time, six concentrations (red dotted lines) were depicted in correlation with the PCR. By calculation, an approximate linear curve in Fig. 5(b) was achieved by the standard equation with an SD less than or equal to 4.5×10^{-6} and an adjusted R^2 equal to 99.15%, which could be described as follows:

$$PCR(\mu\text{A}) = -(67.76 \lg Df_{E.coli} + 29.19), \text{ adjusted } R^2 = 99.15\%, \quad (2)$$

where PCR was the peak current response of the oxidation peak and $\lg Df_{E.coli}$ was the logarithm of the *E. coli* dilution factor. The curve in Fig. 5(b) shows that the linearity of the first point was less

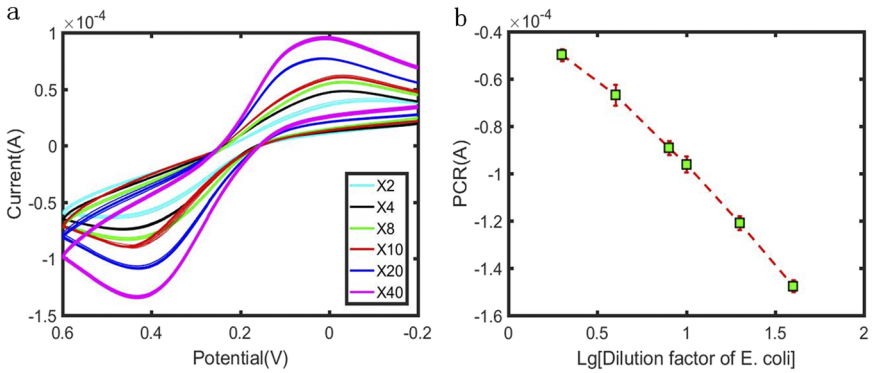

FIG. 5. CV detection curves of *E. coli* solutions with six different dilution factors and the linear standard curve for *E. coli* detection. (a) CV detection curves for *E. coli* measurements. (b) Linear standard curve (the green square points are the averages of the oxidation PCR for different dilution factors; the red solid bars are the SD of the oxidation PCR, n = 10).

ideal because the more limited the sites were for antibody binding to *E. coli*, the more *E. coli* could not be detected, which showed that the upper limit of the PCV system for the detection of the *E. coli* concentration was 5×10^8 cfu/ml. When an *E. coli* solution with an unknown concentration was analyzed, the value of the oxidation or reduction peak in the measured CV curve could be used with the standard equation to calculate the concentration of *E. coli*.

IV. CONCLUSION

In this paper, a PC software-based PCV system with PB-MCNT-GNPs-modified electrodes was developed as a portable, high-performance, and real-time detector for *E. coli* detection using a simple, convenient CV electrochemical detection method and an efficient DPPA algorithm. The accuracy and stability of the PCV system were compared with those of CHI760E; the difference was less than 4.99%, with an RSD less than 0.20%. Based on the PB-MCNT-GNPs composite and antibody-BSA-*E. coli* electrode modification, an electrochemical biosensor was constructed. With effective online processing algorithms such as DPPA, the PCV system could measure the *E. coli* concentration quickly, accurately, and stably with the following standard equation: PCR $= -(67.76 \lg Df_{E.coli} + 29.19)$, adjusted $R^2 = 99.15\%$. A modified electrode was measured by the PCV system at different times for stability testing. The average PCR of the modified electrode was 90.5% after 6 h, and the SD was less than or equal to 3.83×10^{-6}. Six modified electrodes with a diameter of 1 mm were measured at the same time for reproducibility testing. The max difference of the average PCR of six modified electrodes was 4.8×10^{-6} (specific stability and reproducibility data are detailed in the supplementary material, as shown in Figs. S2 and S3). The modified electrode exhibited good stability and reproducibility, which indicated great detection potential for on-site monitoring and met the requirements of real-time and portable detection in various food safety fields. Therefore, a PCV system based on online-adjustable PC software has been successfully constructed and can be used for on-site measurement of *E. coli* and other biomolecules using a PB-MCNT-GNPs-modification method on electrodes.

SUPPLEMENTARY MATERIAL

See the supplementary material for the DPPA algorithm flow chart, stability, and reproducibility data of the PCV system.

ACKNOWLEDGMENTS

This work was supported by the National Natural Science Foundation of China (Grant No. 61871165) and the Public Welfare Project of the Zhejiang Provincial Science and Technology Department (Grant Nos. 2017C33055 and 2016C33078).

REFERENCES

[1] T. Sato, V. V. Plashnitsa, M. Utiyama, and N. Miura, Electrochem. Commun. **12**, 524 (2010).
[2] E. M. Boon, D. M. Ceres, T. G. Drummond, M. G. Hill, and J. K. Barton, Nat. Biotechnol. **18**, 1096 (2000).
[3] Y. C. Wang, D. Cokeliler, and S. Gunasekaran, Electroanalysis **27**, 2527 (2015).
[4] R. G. Bozic and A. C. West, J. Appl. Electrochem. **44**, 293 (2014).
[5] R. Y. Shen, W. M. Zhang, Y. Yuan, G. Y. He, and H. Q. Chen, J. Appl. Electrochem. **45**, 343 (2015).
[6] C. Y. Huang, D. O'Hare, I. J. Chao, H. W. Wei, Y. F. Liang, B. D. Liu, M. H. Lee, and H. Y. Lin, Biosens. Bioelectron. **67**, 208 (2015).
[7] G. M. Alves, J. M. Magalhães, P. Salaün, C. M. G. van den Berg, and H. M. Soares, Anal. Chim. Acta **703**, 1 (2011).
[8] W. Zhang, Y. Xu, X. Zou, and P. Wang, Biosens. Bioelectron. **97**, 267 (2017).
[9] F. Manea, C. Radovan, and J. Schoonman, J. Appl. Electrochem. **36**, 1075 (2006).
[10] R. İnam and C. Bilgin, J. Appl. Electrochem. **43**, 425 (2013).
[11] A. Shamsi, F. Ahour, and B. Sehatnia, J. Solid State Electrochem. **22**, 2681 (2018).
[12] N. H. Giskeødegård, O. Hunderi, and K. Nisancioglu, J. Appl. Electrochem. **48**, 569 (2018).
[13] D. Z. Ji, L. Liu, S. Li, C. Chen, Y. L. Lu, J. J. Wu, and Q. J. Liu, Biosens. Bioelectron. **98**, 449 (2017).
[14] E. S. Friedman, M. A. Rosenbaum, A. W. Lee, D. A. Lipson, B. R. Land, and L. T. Angenent, Biosens. Bioelectron. **32**, 309 (2012).
[15] J. J. Li, Comput. Appl. Chem. **24**, 989 (2007).
[16] E. A. Andreev, M. A. Komkova, V. A. Krupenin, D. E. Presnov, and A. A. Karyakin, Russ. J. Electrochem. **53**, 92 (2017).
[17] H. Narimo, H. Fukuda, and H. Murase, IFAC Proc. Vol. **46**, 261 (2013).
[18] R. Sánchez-Salcedo, R. Miranda-Castro, N. de los Santos-Álvarez, and M. J. Lobo-Castañón, ChemElectroChem **6**, 793 (2019).
[19] K. Kellner, J. Ettenauer, K. Zuser, T. Posnicek, and M. Brandl, Procedia Eng. **168**, 594 (2016).
[20] K. N. Balasubramaniam, B. A. Beisner, J. A. Hubbard, J. J. Vandeleest, E. R. Atwill, and B. McCowan, Anim. Behav. **151**, 131 (2019).
[21] C. Sommers, N. W. Gunther, and S. Sheen, Food Microbiol. **64**, 135 (2017).
[22] G. L. Blay, I. Fliss, and C. Lacroix, J. Microbiol. Methods **59**, 211 (2004).
[23] J. Khang, D. Kim, K. W. Chung, and J. H. Lee, Talanta **147**, 177 (2016).
[24] X. Luo, Y. Zhang, W. Wang, and Y. Cui, J. Instrum. **14**, T01004 (2019).
[25] Z. Q. Shen, J. F. Wang, Z. G. Qiu, M. Jin, X. W. Wang, Z. L. Chen, J. W. Li, and F. H. Cao, Biosens. Bioelectron. **26**, 3376 (2011).
[26] Y. Z. Dou, Z. N. Jiang, W. P. Deng, J. Su, S. X. Chen, H. Y. Song, A. Aldalbahi, X. L. Zuo, S. P. Song, J. Shi, and C. H. Fan, J. Electroanal. Chem. **781**, 339 (2016).
[27] A. Sun, T. Wambach, A. G. Venkatesh, and D. A. Hall, in *IEEE Biomedical Circuits and Systems Conference* (IEEE, 2014), p. 312.
[28] G. Schulze, A. Jirasek, M. L. Yu, A. Lim, R. B. Turner, and M. W. Blades, Appl. Spectrosc. **59**, 545 (2005).
[29] V. Horvat-Radošević and K. Kvastek, J. Electroanal. Chem. **631**, 10 (2009).
[30] S. Buteau, D. C. Dahn, and J. R. Dahn, J. Electrochem. Soc. **165**, A228 (2018).
[31] U. Dharmasiri, M. A. Witek, A. A. Adams, J. K. Osiri, M. L. Hupert, T. S. Bianchi, D. L. Roelke, and S. A. Soper, Anal. Chem. **82**, 2844 (2010).